AIChE WILEY InterScience DISCOVER SOMETHING GREAT

METERIALS, INTERFACES, AND ELECTROCHEMICAL PHENOMENA

Synthesis of Ultrafine Carbon Cryogel Microspheres Using a Homogenizer

Apinan Soottitantawat
National Nanotechnology Center (NANOTEC), National Science and Technonology Development Agency (NSTDA), Klong Luang, Patumthani 12120, Thailand

Takuji Yamamoto, Akira Endo, Takao Ohmori, and Masaru Nakaiwa
Research Institute for Innovation in Sustainable Chemistry, National Institute of Advanced Industrial Science and Technology (AIST), Tsukuba 305-8565, Japan

DOI 10.1002/aic.11053
Published online November 14, 2006 in Wiley InterScience (www.interscience.wiley.com).

Ultrafine carbon cryogel (UCC) microspheres of diameter <5 μm with desirable mesopores were successfully synthesized using a homogenizer during the inverse emulsion polymerization of a resorcinol–formaldehyde (RF) aqueous solution in an organic solvent as a continuous phase (CP) containing nonionic surfactant, SPAN80 as an emulsifier, followed by solvent exchange, freeze-drying, and pyrolysis in an Ar atmosphere. The curing time of RF solution before emulsification is a significant factor in controlling the size of the microspheres without changing their porosity. Both the mesoporosity and the size of the microspheres decreased on increasing SPAN80 and RF solution concentration in an inverse emulsion, which showed the possibility of controlling the mesoporosity and the size of the UCC microspheres. Furthermore, hexane could also be used as the continuous phase in the emulsion polymerization. The mean diameter of the UCC microspheres increased and their mesopore volume decreased with increasing pyrolysis temperature. © 2006 American Institute of Chemical Engineers *AIChE J,* 53: 228–236, 2007
Keywords: carbon microbeads, pyrolysis, adsorption, mesoporous carbon, inverse emulsion

Introduction

Porous materials are used in many chemical processes. Their applications depend on their physical and chemical properties, particularly the pore size. Microporous materials ($r_p < 1$ nm, where r_p is pore radius) are used mainly as adsorbents, taking advantage of their large surface areas and the high adsorptive force of the micropores. Mesoporous materials ($1 < r_p < 25$ nm) generally possess lower surface areas and are less adsorptive than microporous materials, although they do have favorable properties in terms of the ease of mass transfer into the pores, particularly for large molecules.

Many methods have been proposed for the preparation of porous materials, among which sol–gel polycondensation is the most widely used for preparing organic, inorganic, and hybrid organic–inorganic materials. Research on the synthesis of porous materials, particularly those with mesoporosity, has focused mainly on mesostructural diversity, compositional flexibility, and morphological control.

Since the 1990s, resorcinol–formaldehyde (RF) organic gels have received considerable attention as carbon precursors because of their unique properties, such as high surface areas and controlled porous structures.[1] Since the first report by Pekala et al.,[2,3] research has focused on achieving and controlling the

Correspondence concerning this article should be addressed to T. Yamamoto at yamamoto-t@aist.go.jp.

desired mesoporosity of these carbon gels and on modifying the synthesis processes. The carbons produced have been used as thermal and acoustic insulators, adsorbents,[4] chromatographic packings,[5] catalyst supports,[6–9] electrodes,[10–18] and storage systems for hydrogen or methane.[19]

Recently, mesoporous carbon (MC) materials, which are generally prepared by carbonization of precursor gels, have received much attention as a result of their potential applications. To date, MC has been prepared in the form of powders, thin films, and monoliths. The ability to obtain mesoporous particles with a controlled particle size is important for many practical applications. At present, there are two candidate methods for producing MC particles. Spherical MC particles were first successfully prepared by using mesoporous silica particles as templates.[20] Yamamoto et al.[5] recently succeeded in preparing MC microspheres with controlled porous properties through the polymerization of an inverse emulsion of an aqueous RF solution in cyclohexane containing SPAN80 as an emulsifier. The synthesis route involves fewer steps and the MC can be directly prepared from RF solution. A freeze-drying method has also been proposed for the production of mesoporous carbon cryogel microspheres (MCCM). This synthesis method has received attention because of its ability to produce spherical mesoporous carbon particles. Tonanon et al.[21] reported the effects of nonionic and cationic surfactants in the emulsification process on the morphologies and porous properties of the carbons produced. Horikawa et al.[22] reported a way of controlling the size of the carbon microspheres by changing the viscosity of the basic RF sol and the stirring speed; they also reported the effects of the hydrophile–lipophile balance (HLB) values of the nonionic surfactant on the porosity of the carbon microspheres: the pore volume decreased with decreasing HLB value.[23] We previously demonstrated the application of the MC microspheres[4,5] and the effects of the synthesis conditions on the porous properties of the product.[24] The dehydration of RF emulsion particles during the emulsification process and the holding time for the emulsion have significant effects on the porous characteristics of the products. Recently, we also reported on the effect of the drying method on the gas-adsorption characteristics.[25]

The mean sizes of the MC microspheres generally range from 10 to 500 μm. Chromatograms for the separation of benzene, toluene, and *o*-xylene by HPLC show tailing when the mean size of MC microspheres used as the column packing materials is about 50 μm.[5] This problem could be solved by using smaller MC microspheres. The height equivalent to a theoretical plate decreases with decreasing size of the packing material, resulting in improved separation.[27] Smaller MC microspheres are therefore expected to show a number of advantages. For example, ultrafine MC microspheres would be very useful in catalysis and gas adsorption, as they would provide greater pore accessibility and facilitate molecular diffusion.

In this work, attempts were made to prepare ultrafine carbon cryogel microspheres (UCC microspheres; particle diameter $<$ 5 μm) with desired porous properties by the inverse-emulsion polymerization of a RF solution. The size of UCC microspheres was controlled by using a homogenizer and by altering the concentration of the emulsifier, SPAN80. The effects of the conditions for the inverse-emulsion polymerization were examined, particularly the curing time for the RF solution before starting the emulsification process, the mass ratio of SPAN80 to RF solution (M_{SP}/M_{RF}), and the concentration of RF solution in the inverse emulsion, [$M_{RF}/(M_{RF} + M_{CP})$; CP = continuous phase]. Furthermore, because hexane has a low density and is easy to separate from ultrafine RF particle, its use as a replacement for cyclohexane as the continuous phase for the emulsion was also examined.

Experimental

Materials

Resorcinol, formaldehyde (37%; methanol stabilized), and sodium carbonate (Na_2CO_3) used in the sol–gel polycondensation were purchased from Wako Pure Chemical Industries, Ltd. (Osaka, Japan) in research grade chemicals. Distilled and ion-exchanged water was used as a diluent for the sol–gel polycondensation. In the emulsion process, the following reagents were used: cyclohexane, hexane, SPAN80. All were also purchased from Wako in research grade. Further, *t*-butanol was used in the freeze-drying process from Wako in research grade.

Preparation of ultrafine RF hydrogel microspheres

RF hydrogels were synthesized by the polycondensation of resorcinol (R) and formaldehyde (F), by using sodium carbonate as a basic catalyst (C). The RF solutions contained resorcinol, formaldehyde, sodium carbonate, and pure water (W). The molar ratio of resorcinol to catalyst (R/C) was fixed at 400, the ratio of resorcinol to water (R/W) was fixed at 0.25 g/cm^3, and the molar ratio of resorcinol to formaldehyde (R/F) was fixed at 0.5. The prepared RF solutions were kept at 298 K and the sol–gel transition was allowed to proceed before starting the emulsification. At a certain reaction time, the size distribution of the colloidal particles formed in the RF solution was measured by dynamic light scattering (DLS) (LB-550, Horiba, Kyoto, Japan). Further, a transient change of the viscosity of the RF solution during the sol–gel polycondensation was measured at 298 K using an Ostwald viscosity meter.

The particles were then dispersed into the organic continuous phase (CP: cyclohexane or hexane) containing SPAN80 as surfactant. The concentration of RF solution in the CP [$M_{RF}/(M_{RF} + M_{CP})$] and the ratio of SPAN80 to RF solution (M_{SP}/M_{RF}) were varied over the ranges 0.20–0.50 and 0.10–1.00, respectively (Table 1). The inverse emulsion was formed by using a homogenizer at 15,000 rpm for 3 min at room temperature. The emulsion was subsequently stirred at 200 rpm at room temperature for 1 week to complete the sol–gel polycondensation and to obtain ultrafine RF hydrogel microspheres (URH microspheres).

Preparation of ultrafine RF cryogel microspheres

The URH microspheres were separated from the continuous phase by centrifugation (High Speed Refrigerated Centrifuge SRX-201, Tomy Seiko Co., Ltd., Tokyo, Japan) at 12,000 rpm (26,568 g-force) for 10 min. After the continuous phase had been removed, the URH microspheres obtained were immersed in *t*-butanol for 24 h to exchange the water in the hydrogels with *t*-butanol and then centrifuged at 12,000 rpm for 15 min. This process was repeated three times. The microspheres were kept at 243 K for 1 day, and then dried under a vacuum at 263 K for 4 days to obtain ultrafine RF cryogel microspheres (URC microspheres).

Table 1. Conditions for the Inverse Emulsion Polymerization of RF Solutions, Characteristic Size of URH Microspheres, and Porous Properties of URC Microspheres

Continuous Phase	Curing Time* (h)	$\frac{M_{RF}}{(M_{RF}+M_{CP})}$	$\frac{M_{SP}}{M_{RF}}$	Mean Size (μm)	SD** (μm)	S_{BET} (m^2/g)	V_{mes} (cm^3/g)	r_{peak} (nm)	V_{mic} (cm^3/g)
Cyclohexane†	0	0.20	0.25	3.61	2.20	397	1.06	6.06	0.12
		0.20	0.50	2.97	1.90	379	0.81	4.63	0.12
		0.20	1.00	3.32	2.07	372	0.65	2.41	0.12
	6	0.20	0.25	2.43	0.90	383	1.05	6.06	0.12
		0.20	0.50	2.20	0.94	385	0.77	3.55	0.14
		0.20	1.00	1.82	0.64	334	0.50	2.13	0.13
	9	0.20	0.25	2.01	0.60	389	0.96	4.63	0.13
		0.20	0.50	1.59	0.45	384	0.79	3.55	0.13
		0.20	1.00	1.32	0.38	362	0.56	2.41	0.12
	15	0.20	0.10	5.23	2.94	355	1.10	6.94	0.12
		0.20	0.25	3.43	1.92	374	0.96	6.06	0.14
		0.20	0.50	2.93	1.93	368	0.69	3.55	0.12
		0.20	0.75	1.84	0.55	363	0.58	2.41	0.11
		0.20	1.00	1.66	0.50	342	0.50	2.13	0.11
		0.30	0.25	2.58	3.48	362	0.81	4.05	0.12
		0.40	0.25	1.32	0.54	312	0.67	3.12	0.11
		0.50	0.25	0.60	0.67	196	0.40	2.13	0.08
	24	0.20	0.25	2.48	1.15	384	0.91	4.63	0.14
		0.20	0.50	1.90	0.65	376	0.70	3.12	0.12
		0.20	1.00	2.01	0.75	398	0.61	2.41	0.12
	32	0.20	0.25	3.02	1.56	379	1.00	6.06	0.12
		0.20	0.50	4.74	2.03	390	0.76	4.63	0.12
		0.20	1.00	6.15	2.24	375	0.55	2.74	0.12
Hexane††	15	0.20	0.25	4.06	2.09	388	0.78	4.05	0.12

*Curing time before the emulsification.
**Standard deviation.
†Insoluble in water; density 0.778 g/cm^3 at 20°C.[26]
††Soluble in water; 0.014 g/100 g water; density 0.659 g/cm^3 at 20°C.[26]

Preparation of ultrafine carbon cryogel microspheres

The UCC microspheres were prepared by pyrolyzing the URC microspheres at temperatures (T_{pyro}) of 773, 1073, or 1273 K. Pyrolysis was conducted under a constant argon gas flow of 100 cm^3 (STP)/min. The URC microspheres were initially heated to 523 K at a constant heating rate of 250 K/h, kept at this temperature for 2 h, heated to the desired T_{pyro} at a constant heating rate of 250 K/h, and kept at T_{pyro} for 4 h.

Characterization of the microspheres

The shapes and sizes of URC and UCC microspheres were examined by using a scanning electron microscope (S-3400N, SEM-Hitachi Ltd., Ibaraki, Japan).

The particle size distributions of URH and UCC microspheres were measured by a laser-diffraction particle-size analyzer (Partica LA-950, Horiba, Ltd., Kyoto, Japan). In this study, the size of the URH microspheres was measured rather than that of the URC microspheres to avoid the agglomeration of the microspheres that could occur during the centrifuging and drying of the URH microspheres. Cyclohexane was used as a disperse phase in measuring the size of the URH emulsion. At the point of the measurement, the UCC microspheres were dispersed in distilled water at 0.10 wt % and subjected to sonication for 20 min. The particle size distribution was measured based on the surface area of the particle. The Sauter mean diameter, d_{32}, was then calculated. The standard deviations of the particle-size distributions were also determined.

The porous properties of the URC and UCC microspheres were examined by nitrogen-adsorption experiments using an adsorption apparatus (Belsorp Mini, Bel Japan Inc., Osaka, Japan). After the pretreatment, the adsorption and desorption isotherms of nitrogen were measured at 77 K. The BET (Brunauer–Emmett–Teller) surface areas, the mesopore volumes, and the micropore volumes of the samples were evaluated on the basis of the nitrogen adsorption isotherms. The mesopore size distributions were determined by applying the Dollimore–Heal methods to the desorption isotherms.[28]

Results and Discussion

Effect of the curing time before starting the emulsification on the characteristics of URC microspheres

In this study, we examined the effects of the size of the colloidal particles on the distribution of URC microsphere sizes and its porous properties; together with the viscosity of the RF solution,[22] the size of the colloidal particles was expected to control the size of the UCC microspheres. Under the conditions used in the study (C/W = 6.25×10^{-4} g/cm^3), the values of t^* (the time that the size distribution of the colloidal particles changed from unimodal to bimodal) and t_{gel} (the gelation time) were about 40 and 48 h, respectively.[28] Figure 1a shows the growth of the colloidal particles as a function of the polymerization time up to 32 h (before the t^*): according to a previous report, the size distribution of colloidal particles is unimodal before t^*. Our previous work[29] reports on the growth of colloidal particles during the early stages of the sol–gel transition as a function of the polymerization time. t^* was also investigated in relation to the composition of the RF solution. This bimodal distribution time indicates when the nucleation and growth of polymer clusters is nearly complete and interconnection of the colloidal particles has started.[3,28] The interconnection between the colloidal particles after t^*

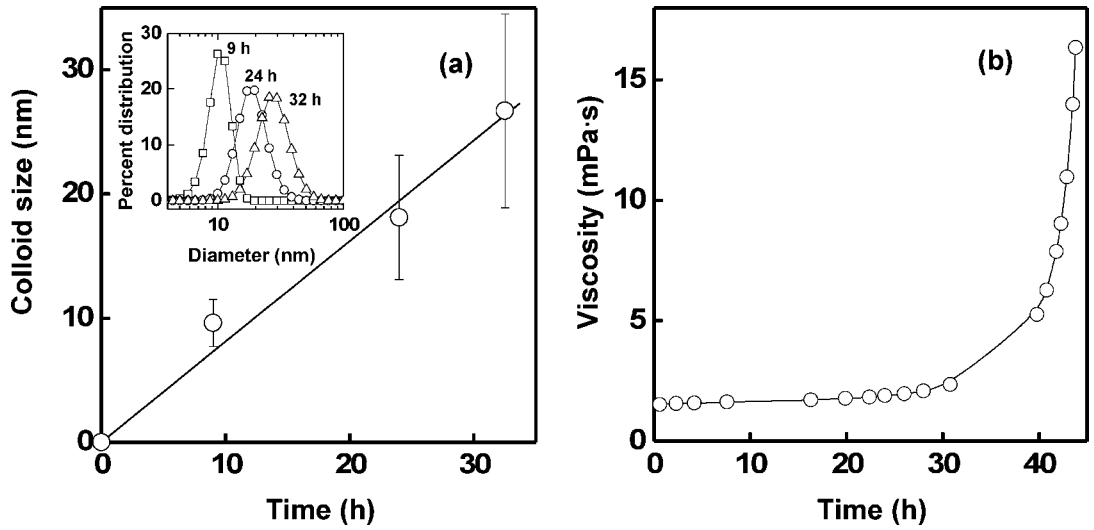

Figure 1. Mean size of colloidal particle and viscosity of a RF solution.

Transient changes of the size of colloidal particles formed in a RF solution (a) and viscosity of a RF solution (b) at 298 K.

results in the rapid increase in the viscosity of RF solution, as shown in Figure 1b.

Figure 2 shows the effect of the curing time of a RF solution before starting the emulsification on the size distribution of URH microspheres. The size of URH microspheres was not affected by the curing time that emulsification was performed during the early stage of polymerization, but the size of the URH microspheres obviously increased when emulsification was performed after 32 h. This might be explained by an increase in the viscosity of the RF solution as shown in Figure 1b, which was also mentioned by Horikawa et al.[22] Note that most of the microsphere sizes were in the range 1–5 μm and the size strongly depended on the curing time. SEM images of URC microspheres are shown in Figure 3 as a function of the curing time: the URC microspheres have spherical shapes.

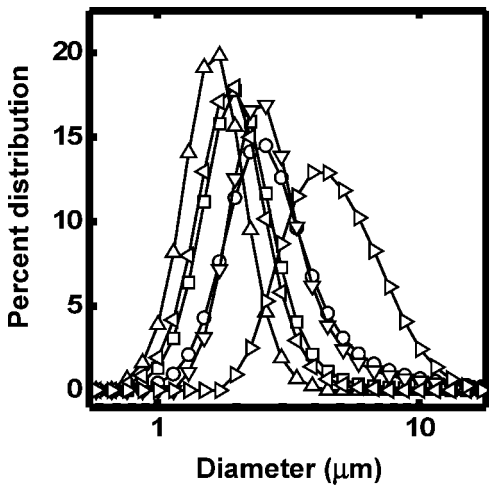

Figure 2. Size distribution of URH microspheres.

Keys: curing time before the emulsification process (○) 0 h, (□) 6 h, (△) 9 h, (▽) 15 h, (◁) 24 h, (▷) 32 h. CP: cyclohexane, $M_{RF}/(M_{RF} + M_{CP}) = 0.20$, $M_{SP}/M_{RF} = 0.50$.

Partial agglomeration of the URC microspheres, which occurred during the centrifuging and drying processes, could be observed. The size of cryogel microspheres was <1 μm when emulsification was performed before 24 h of curing time. The size was >1 μm for emulsification at a curing time of 32 h. Furthermore, the size of URC microspheres was smaller than the URH microspheres, as shown in Figure 3, because of the shrinkage that occurred during drying.

Adsorption and desorption isotherms of nitrogen on the URC microspheres are shown in Figure 4. The isotherms are of Type IV (IUPAC classification), which indicates the development of mesoporosity in the samples, and the mesopore volumes were significantly larger than the micropore volumes. The adsorption and desorption isotherms did not show any significant dependency on the curing time or size of colloid particle, for all the M_{SP}/M_{RF} ratios studied. The mesopore size distributions of URC microspheres were not changed and the pore sizes were almost constant, irrespective of the curing time.

The porous properties of the URC microspheres are shown in Table 1. In all systems, the BET surface area was approximately 380 m^2/g. The mesopore volumes were also unchanged on

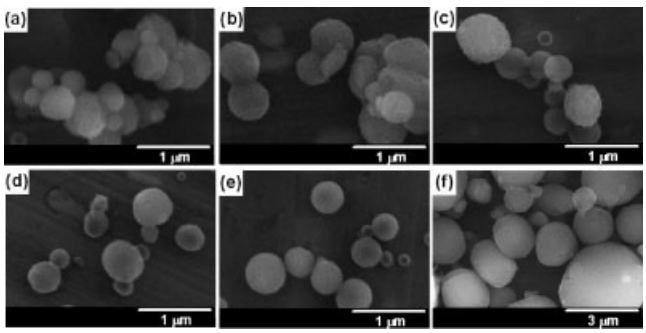

Figure 3. SEM images of URC microspheres.

CP: cyclohexane, $M_{RF}/(M_{RF} + M_{CP}) = 0.20$, M_{SP}/M_{RF} of 0.50: (a) 0 h, (b) 6 h, (c) 9 h, (d) 15 h, (e) 24 h, (f) 32 h.

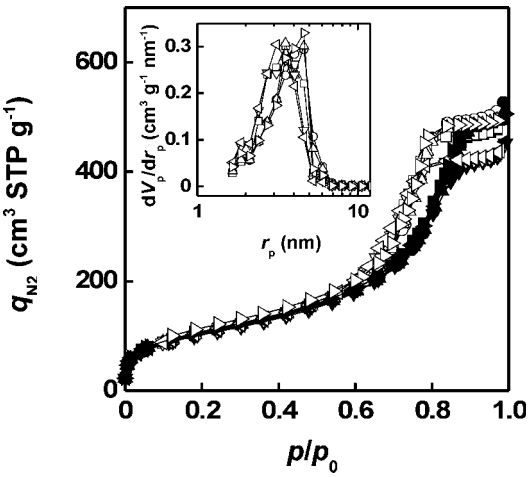

Figure 4. N_2 adsorption/desorption isotherms at 77 K and pore size distribution curves of URC microspheres.

CP: cyclohexane, $M_{RF}/(M_{RF} + M_{CP}) = 0.20$, $M_{SP}/M_{RF} = 0.50$; closed symbols: adsorption; open symbols: desorption. Keys: curing time before the emulsification: (○) 0 h, (□) 6 h, (△) 9 h, (▽) 15 h, (◁) 24 h, (▷) 32 h.

increasing the curing time. Thus, the curing time is confirmed to be an important factor for controlling the particle size of the URC microspheres without changing their porous properties.

Effect of SPAN80 concentration on the characteristics of URC microspheres

In all emulsification processes, the ratio of the surfactant to the dispersed phase is a significant factor in controlling the size of the dispersed phase. Figure 5 shows the Sauter mean diameter and the size distribution of URH microspheres as functions of the SPAN80 concentration (M_{SP}/M_{RF}). The size distribution curve shifted to a smaller range on increasing the value of M_{SP}/M_{RF}. The mean diameter also decreased on increasing the value of M_{SP}/M_{RF}. The maximum and minimum mean diameters of URH microspheres were about 5 and 1.5 μm for M_{SP}/M_{RF} ratios of 0.10 and 1.00, respectively. SEM studies showed that the URC microspheres also have a spherical shape (Figure 6). It should be noted that the size of URC microspheres was smaller than that of URH microspheres as discussed in the previous section. However, for emulsification of the high-viscosity RF solution at a polymerization time of 32 h, the mean size of the URH microspheres increased with increasing M_{SP}/M_{RF} (Table 1). This indicates that, at a long curing time, the viscosity of a RF solution is a more significant factor than M_{SP}/M_{RF}, which determines the surface tension between the RF solution and cyclohexane containing SPAN80, in controlling the size of the microspheres.

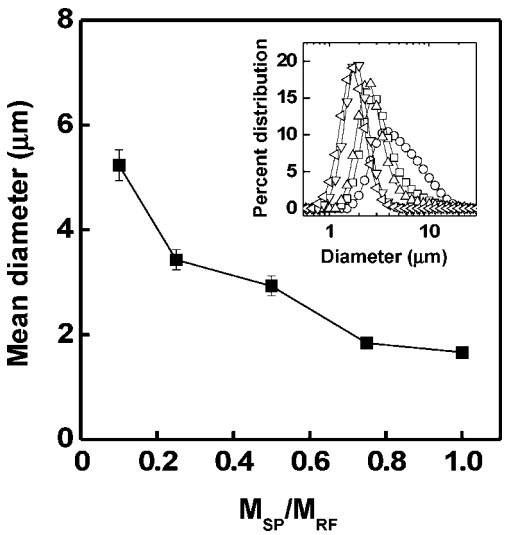

Figure 5. Mean size and size distribution of URH microspheres.

The error bars show standard error of means. CP: cyclohexane, $M_{RF}/(M_{RF} + M_{CP}) = 0.20$, curing time = 15 h. Keys: M_{SP}/M_{RF} (○) 0.10, (□) 0.25, (△) 0.50, (▽) 0.75, (◁) 1.00.

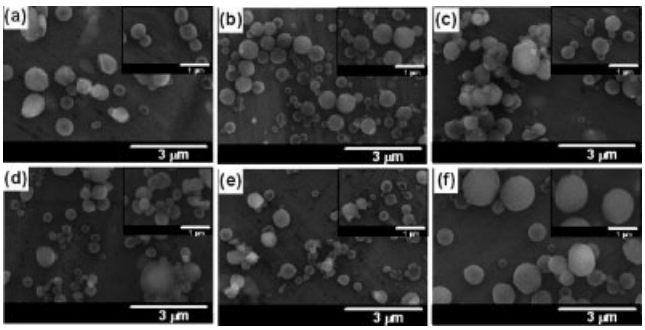

Figure 6. SEM images of the obtained URC microspheres.

$M_{RF}/(M_{RF} + M_{CP}) = 0.20$, curing time = 15 h. CP: cyclohexane: (a) $M_{SP}/M_{RF} = 0.10$, (b) 0.25, (c) 0.50, (d) 0.75, (e) 1.00, (f) $M_{SP}/M_{RF} = 0.25$ with CP: hexane.

The effects of M_{SP}/M_{RF} on the adsorption and desorption isotherms of nitrogen and mesopore size distribution of the

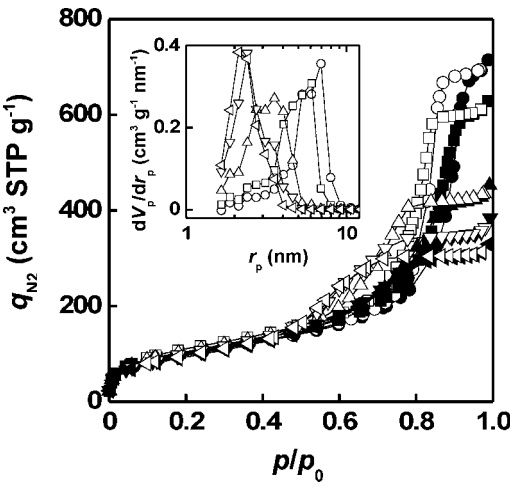

Figure 7. N_2 adsorption/desorption isotherms at 77 K and pore size distribution curves of URC microspheres.

CP: cyclohexane, $M_{RF}/(M_{RF} + M_{CP}) = 0.20$, curing time = 15 h; closed symbols: adsorption; open symbols: desorption. Keys: M_{SP}/M_{RF} (○) 0.10, (□) 0.25, (△) 0.50, (▽) 0.75, (◁) 1.00.

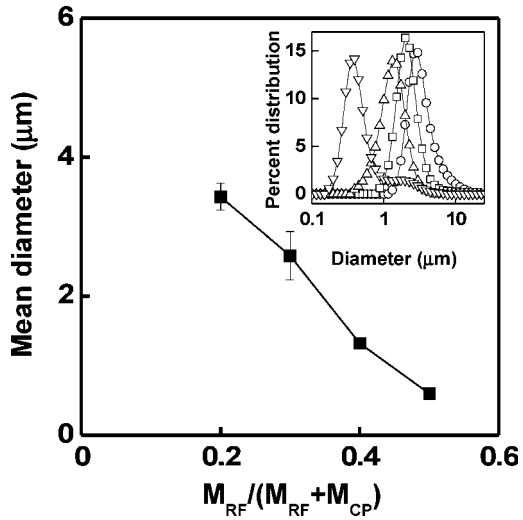

Figure 8. Mean size and size distribution of URH microspheres.

The error bars show standard error of means. CP: cyclohexane, $M_{SP}/M_{RF} = 0.25$, curing time = 15 h. Keys: $M_{RF}/(M_{RF} + M_{CP})$ (○) 0.20, (□) 0.30, (△) 0.40, (▽) 0.50.

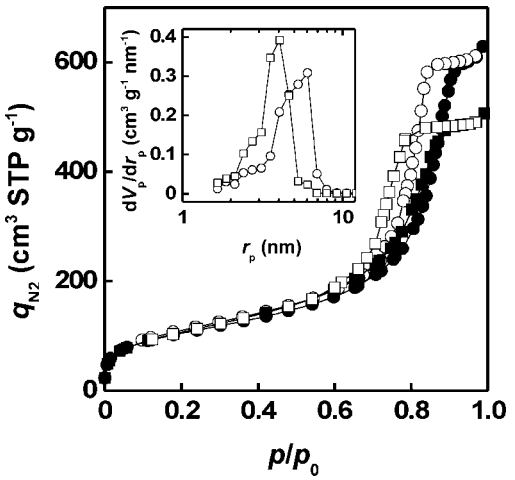

Figure 10. N_2 adsorption/desorption isotherms at 77 K and pore size distribution curves of URC microspheres.

$M_{RF}/(M_{RF} + M_{CP}) = 0.20$, $M_{SP}/M_{RF} = 0.25$, curing time = 15 h; closed symbols: adsorption; open symbols: desorption. Keys: CP (○) Cyclohexane, (□) hexane.

URC microspheres are shown in Figure 7. The peak radius of the mesopore size distribution decreased with increasing M_{SP}/M_{RF}. The porous properties of URC microspheres are also shown in Table 1. The peak radii of the mesopore size distribution were 6.94, 6.06, 3.55, 2.41, and 2.13 nm at 15 h of curing time before the emulsification in cyclohexane for values of M_{SP}/M_{RF} of 0.10, 0.25, 0.50, 0.75, and 1.00, respectively. The mesopore volumes also decreased with increasing M_{SP}/M_{RF}. This could be explained by increased dehydration resulting from the higher SPAN80 concentration, as reported by Yamamoto et al.[24] The higher dehydration indicates a greater loss of water molecules from the network, which leads to a shrinkage of the porous structure of the URC microspheres. The BET surface area and the micropore volume were unaffected by the value of the M_{SP}/M_{RF} ratio.

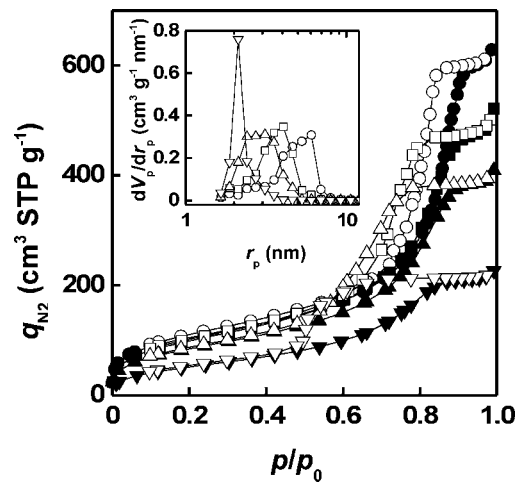

Figure 9. N_2 adsorption/desorption isotherms at 77 K and pore size distribution curves of URC microspheres.

CP: cyclohexane, $M_{SP}/M_{RF} = 0.25$, curing time = 15 h; closed symbols: adsorption; open symbols: desorption. Keys: $M_{RF}/(M_{RF} + M_{CP})$ (○) 0.20, (□) 0.30, (△) 0.40, (▽) 0.50.

Effect of the ratio of the RF solution and cyclohexane on the characteristics of URC microspheres

Figure 8 shows the effect of the concentration of the RF solution in cyclohexane [$M_{RF}/(M_{RF} + M_{CP})$] on the size distribution and the Sauter mean diameter of the URH microspheres. The Sauter mean diameter decreased with the increasing RF concentration. The mean diameter was about 3.50 and 0.30 μm at $M_{RF}/(M_{RF} + M_{CP})$ ratios of 0.20 and 0.50, respectively.

The adsorption and desorption isotherms of nitrogen on the URC microspheres (Figure 9) show an effect of the $M_{RF}/(M_{RF} + M_{CP})$ ratio. The isotherms are of type IV. The mesopore size distribution of URC microspheres is also shown in Figure 9. The peak radius of the mesopore size distribution decreased with the increasing $M_{RF}/(M_{RF} + M_{CP})$ ratio. The porous properties are also shown in Table 1. The BET surface area and mesopore volume decreased with increasing RF solution concentration in the emulsion. This might be explained by the increasing of surface area of the smaller particles in the higher concentration of RF solutions, resulting in the higher

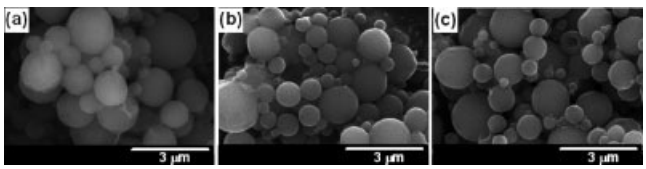

Figure 11. SEM images of UCC microspheres.

(a) T_{pyro} 773 K, (b) 1073 K, (c) 1273 K. CP: cyclohexane, $M_{SP}/M_{RF} = 0.25$, $M_{RF}/(M_{RF} + M_{CP}) = 0.20$, curing time = 32 h.

Table 2. Characteristic Sizes and Porous Properties of UCC Microspheres at Different Pyrolysis Temperatures and SPAN80 Concentrations

Continuous Phase	Curing Time* (h)	T_{pyro} (K)	$\frac{M_{RF}}{(M_{RF}+M_{CP})}$	$\frac{M_{SP}}{M_{RF}}$	Mean Size (μm)	SD[b] (μm)	S_{BET} (m^2/g)	V_{mes} (cm^3/g)	r_{peak} (nm)	V_{mic} (cm^3/g)
Cyclohexane	32	723	0.20	0.25	3.94	2.10	672	0.87	4.63	0.22
		1073	0.20	0.25	5.51	2.19	692	0.75	4.05	0.29
		1273	0.20	0.25	5.59	2.33	649	0.72	4.05	0.29
		1273	0.20	0.50	4.32	1.87	649	0.47	2.74	0.29
		1273	0.20	1.00	5.40	2.14	574	0.27	1.88	0.26

*Curing time before the emulsification.

dehydration from the network that leads to a shrinkage of the porous structure.

Characteristics of URC microspheres when hexane was used as the continuous phase in the inverse-emulsion polymerization

The effects of replacing cyclohexane with hexane as a continuous phase in the inverse emulsion were examined. The URH microspheres obtained by using hexane as the CP were larger than those prepared by using cyclohexane as the CP (Table 1). The surface tensions between hexane–water and cyclohexane–water were almost the same. Therefore, this result might be caused by the differences between the densities of hexane and cyclohexane as shown in Table 1. The shape of the URC microspheres was also spherical (Figure 6f). In relation to the porous properties, type IV adsorption–desorption isotherms were also observed with hexane as the CP (Figure 10). The mesopore size distributions are also shown in Figure 10. A larger mesopore size was observed with cyclohexane as the CP compared with hexane. In addition, the mesopore volume was smaller with hexane as CP (Table 1). This could be explained by the greater degree of removal of water from the inside of particle sol–gels to the hexane CP, arising from the higher solubility of hexane in water than that of cyclohexane, as shown in Table 1. The BET surface area and micropore volume, however, were similar to those of URC microspheres synthesized by using cyclohexane as CP. This shows that hexane, a cheaper solvent than cyclohexane, can be used as the CP in the inverse-emulsion polymerization process, a result that is favorable from the perspective of scaling up the production process for URC or UCC microspheres.

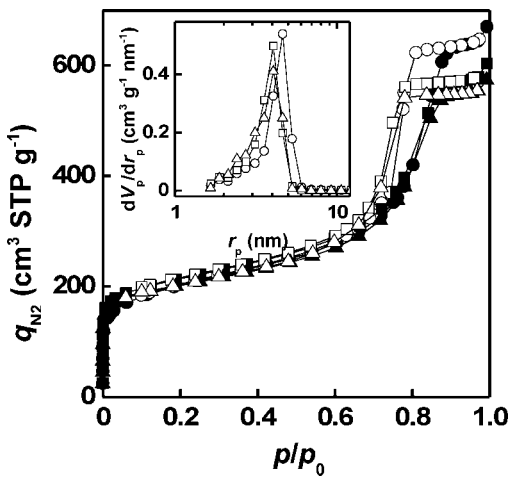

Figure 12. N_2 adsorption/desorption isotherms at 77 K and pore size distribution curves of URC microspheres.

CP: cyclohexane, $M_{SP}/M_{RF} = 0.25$, $M_{RF}/(M_{RF} + M_{CP}) = 0.20$, curing time = 32 h; closed symbols: adsorption; open symbols: desorption. Keys: T_{pyro} (○) 773 K, (□) 1073 K, (△) 1273 K.

The effect of the pyrolysis temperature on the characteristics of UCC microspheres

Figure 11 shows the SEM image of UCC microspheres. The spherical shape was maintained after pyrolysis. The mean size of UCC microspheres increased with increasing pyrolysis temperature (Table 2). This could be explained by the agglomeration of small particles at higher pyrolysis temperatures.

Type IV adsorption–desorption isotherms were also observed after the pyrolysis, and the mesopore size and mesopore volume decreased with increasing pyrolysis temperature (Figure 12 and Table 2), which agreed with the results reported by Hanzawa et al.[30] The mesopore volume decreased with increasing pyrolysis temperature because of the fusion of the primary particles forming the network structure of the carbon cryogels. The BET surface area and micropore volume of the UCC microspheres were confirmed to be twice those of the URC microspheres.

Furthermore, the size and the volume of the mesopores of the UCC microspheres decrease with the increasing M_{SP}/M_{RF} (Table 2), whereas the BET surface area and micropore volume were scarcely affected by the value of M_{SP}/M_{RF}. The effect of the SPAN80 concentration on the porous properties of UCC microspheres was the same as the effect on the URC microspheres, as discussed earlier. The mean size of these UCC microspheres was not affected by SPAN80 concentration. This could be explained, for emulsification at 32 h of

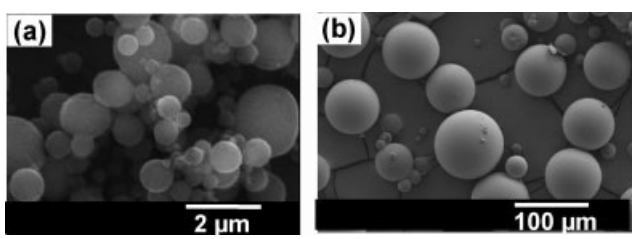

Figure 13. SEM images of UCC microspheres and CC microspheres.

CP: cyclohexane, $M_{SP}/M_{RF} = 0.25$, $M_{RF}/(M_{RF} + M_{CP}) = 0.20$, curing time = 32 h, $T_{pyro} = 1273$ K. (a) UCC microspheres, (b) CC microspheres.

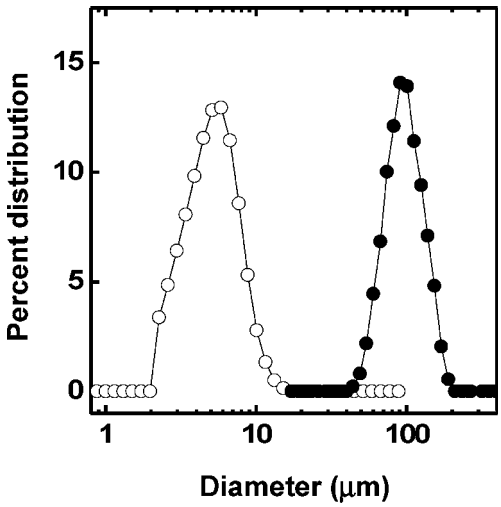

Figure 14. Size distribution of UCC microspheres and CC microspheres.

CP: cyclohexane, $M_{SP}/M_{RF} = 0.25$, $M_{RF}/(M_{RF} + M_{CP}) = 0.20$, curing time = 32 h, $T_{pyro} = 1273$ K. Keys: (○) UCC microspheres, (●) CC microspheres.

curing time, by the fact that the viscosity of a RF solution is a more significant factor than the concentration of SPAN80 in controlling the size of the microspheres as discussed in the previous section.

Comparison of UCC microspheres with CC microspheres

Figure 13 shows the images of UCC microspheres synthesized using a homogenizer and CC (carbon cryogel) microspheres synthesized without using a homogenizer as reported in our previous work.[24] It can be seen that UCC microspheres possess much smaller particle diameters compared to those of the CC microspheres, as shown in Figure 14. This is because the size of the emulsion can be effectively decreased by the high-speed agitation using a homogenizer. Furthermore, any differences between the porous characteristics of either UCC or CC microspheres are dependent on the content of water, catalyst in RF solution,[5] the amount of SPAN80 during the emulsification process, and the pyrolysis temperature as explained above.

Conclusions

Ultrafine carbon cryogel microspheres with a spherical shape and developed mesoporosity were obtained by inverse-emulsion polymerization of RF aqueous solutions in an organic continuous phase containing SPAN80 as an emulsifier, followed by freeze-drying and pyrolysis in an inert atmosphere. The key to this synthetic route is the use of a homogenizer during the inverse-emulsion polymerization. The size of UCC microspheres was in the range 0.50–5 μm, depending on the concentrations of SPAN80 and RF solution in the emulsion, which was much smaller than the CC microspheres synthesized without using a homogenizer. The porous properties of the UCC microspheres could be effectively controlled by changing the concentrations of SPAN80 and the RF solution, and by changing the organic solvent to hexane. This novel method provides opportunities for the synthesis of the ultrafine carbon gel microspheres with desired levels of mesoporosity and controlled particle sizes. This method is believed to be applicable to the large-scale production of ultrafine carbon microspheres, which will be examined in our future work.

Acknowledgments

The authors are grateful for financial support from the New Energy and Industrial Technology Development Organization (NEDO) and the Japanese Ministry of Education, Culture, Sports, Science and Technology, Grant-in-Aid for Scientific Research.

Literature Cited

1. Al-Muhtaseb SA, Ritter JA. Preparation and properties of resorcinol-formaldehyde organic and carbon gels. *Adv Mater*. 2003;15:101–114.
2. Pekala RW. Organic aerogel from the polycondensation of resorcinol with formaldehyde. *J Mater Sci*. 1989;24:3221–3227.
3. Pekala RW, Kong FM. A synthetic route to organic aerogels—Mechanism, structure, and properties. *Rev Phys Appl*. 1989;C4:33–40.
4. Yamamoto T, Endo A, Ohmori T, Nakaiwa M. Porous properties of carbon gel microspheres as adsorbents for gas separation. *Carbon*. 2004;42:1671–1676.
5. Yamamoto T, Sugimoto T, Suzuki T, Mukai SR, Tamon H. Preparation and characterization of carbon cryogel microspheres. *Carbon*. 2002;40:1345–1351.
6. Mukai SR, Sugiyama T, Tamon H. Immobilization of heteropoly acids in the network structure of carbon gels. *Appl Catal A*. 2003;256: 99–105.
7. Moreno-Castilla C, Maldonado-Hodar FJ, Perez-Cadenas AF. Physicochemical surface properties of FE, Co, Ni, and Cu-doped monolithic organic aerogels. *Langmuir*. 2003;19:5650–5655.
8. Job N, Pirard R, Marien J, Pirard JP. Synthesis of transition metal-doped carbon xerogels by solubilization of metal salts in resorcinol-formaldehyde aqueous solution. *Carbon*. 2004;42:3217–3227.
9. Smirnova A, Dong X, Hara H, Vasiliev A, Sammes N. Novel carbon-aerogel supported catalysts for PEM fuel cell application. *Int J Hydrogen Energy*. 2005;30:149–158.
10. Pekala RW, Farmer JC, Alviso CT, Tran TD, Mayer ST, Miller JM, Dunn B. Carbon aerogels for electrochemical applications. *J Non-Cryst Solids*. 1998;225:74–80.
11. Saliger R, Fischer U, Herta C, Fricke J. High surface area carbon aerogel for supercapacitors. *J Non-Cryst Solids*. 1998;225:335–342.
12. Lin C, Ritter JA, Popov BN. Correlation of double-layer capacitance with the pore structure of sol–gel derived carbon xerogels. *J Electrochem Soc*. 1999;146:3639–3643.
13. Pröbstle H, Schmitt C, Fricke J. Button cell supercapacitors with monolithic carbon aerogels, J *Power Sources*. 2002;105:189–194.
14. Pröbstle H, Wiener M, Fricke J. Carbon aerogels for electrochemical double layer capacitors. *J Porous Mater*. 2003;10:213–222.
15. Hwang SW, Hyun SH. Capacitance control of carbon aerogel electrodes. *J Non-Cryst Solids*. 2004;347:238–245.
16. Hasegawa T, Mukai SR, Shirato Y, Tamon H. Preparation of carbon gel microspheres containing silicon powder for lithium ion battery anodes. *Carbon*. 2004;42:2573–2579.
17. Alcantara R, Lavela P, Ortiz GF, Tirado JL. Carbon microspheres obtained from resorcinol-formaldehyde as high-capacity electrodes for sodium-ion batteries. *Electrochem Solid State Lett*. 2005;8:A222–A225.
18. Kim SJ, Hwang SW, Hyun SH. Preparation of carbon aerogel electrodes for supercapacitor and their electrochemical characteristics. *J Mater Sci*. 2005;40:725–731.
19. Feaver A, Cao GZ. Activated carbon cryogels for low pressure methane storage. *Carbon*. 2006;44:590–593.
20. Ryoo R, Joo SH, Jun S. Synthesis of highly ordered carbon molecular sieves via template-mediated structural transformation. *J Phys Chem B*. 1999;103:7743–7746.
21. Tonanon N, Tanthapanichakoon W, Yamamoto T, Nishihara H, Mukai SR, Tamon H. Influence of surfactants on porous properties of carbon cryogels prepared by sol–gel polycondensation of resorcinol and formaldehyde. *Carbon*. 2003;41:2981–2990.

22. Horikawa T, Hayashi J, Muroyama K. Size control and characterization of spherical carbon aerogel particles from resorcinol formaldehyde resin. *Carbon*. 2004;42:169–175.
23. Horikawa T, Ono Y, Hayashi J, Muroyama K. Influence of surface-active agents on pore characteristics of the generated spherical resorcinol-formaldehyde based carbon aerogels. *Carbon*. 2004;42:2683–2689.
24. Yamamoto T, Endo A, Ohmori T, Nakaiwa M. The effects of different synthetic conditions on the porous properties of carbon cryogel microspheres. *Carbon*. 2005;43:1231–1238.
25. Yamamoto T, Endo A, Ohmori T, Nakaiwa M, Mukai SR, Tamon H. Effect of drying method on gas adsorption characteristics of carbon gel microspheres. *Drying Technol*. 2005;23:2119–2129.
26. Perry RH, Green DW. *Perry's Chemical Engineer' Handbook*. New York: McGraw-Hill; 1997.
27. Jerkovich AD, Mellors JS, Jorgenson JW. The use of micrometer-sized particles in ultrahigh pressure liquid chromatography. *LCGC North Am*. 2003;21:600–610.
28. Dollimore D, Heal. GR. An improved method for the calculation of pore-size distribution from adsorption data. *J Appl Chem*. 1964;60:235–241.
29. Yamamoto T, Yoshida T, Suzuki T, Tamon H. Dynamic and static light scattering study on the sol–gel transition of resorcinol-formaldehyde aqueous solution. *J Colloid Interface Sci*. 2002;245:391–396.
30. Hanzawa Y, Hatori H, Yoshizawa N, Yamada Y. Structural changes in carbon aerogels with high temperature treatment. *Carbon*. 2002;40:575–581.

Manuscript received May 23, 2006, and revision received Oct. 4, 2006.